Self-calibration wavelength modulation spectroscopy for acetylene detection based on tunable diode laser absorption spectroscopy*

Qin-Bin Huang(黄秦斌), Xue-Mei Xu(许雪梅)†, Chen-Jing Li(李晨静), Yi-Peng Ding(丁一鹏), Can Cao(曹粲), Lin-Zi Yin(尹林子), and Jia-Feng Ding(丁家峰)

School of Physics and Electronics, Central South University, Changsha 410083, *China*

(Received 9 March 2016; revised manuscript received 16 May 2016; published online 30 September 2016)

The expressions of the second harmonic (2f) signal are derived on the basis of absorption spectral and lock-in theories. A parametric study indicates that the phase shift between the intensity and wavelength modulation makes a great contribution to the 2f signal. A self-calibration wavelength modulation spectroscopy (WMS) method based on tunable diode laser absorption spectroscopy (TDLAS) is applied, combining the advantages of ambient pressure, temperature suppression, and phase-shift influences elimination. Species concentration is retrieved simultaneously from selected 2f signal pairs of measured and reference WMS-2f spectra. The absorption line of acetylene (C_2H_2) at 1530.36 nm near-infrared is selected to detect C_2H_2 concentrations in the range of 0–400 ppmv. System sensitivity, detection precision and limit are markedly improved, demonstrating that the self-calibration method has better detecting performance than the conventional WMS.

Keywords: wavelength modulation spectroscopy, phase shift, self-calibration method, acetylene detection

PACS: 42.30.Rx, 42.55.Px, 42.79.–e, 42.87.–d **DOI:** 10.1088/1674-1056/25/11/114202

1. Introduction

C_2H_2, a species of toxic gases, has strong chemical activity and is easy to be decomposed, burn, and explode. In modern energy systems, C_2H_2 is one of the main components of the oil-decomposed fault gases in transformer.[1,2] During the research of plant growth, C_2H_2 can be used as a kind of plant hormone to ripen the fruits or wither the flowers. Therefore, there is a demand for the trace C_2H_2 detection in some practical applications.

Designing rapid and accurate trace gas measurements has become a hot topic. Numerous efforts have been contributed, such as photoacoustic spectrometry (PAS),[3] QEPAS (quartz-enhanced) with a new PAS technique,[4] metal oxide semiconductor (MOS),[5] and TDLAS,[6,7] among these methods, the TDLAS technique has been frequently used due to its high sensitivity and accuracy. In order to further improve the signal to noise rate (SNR), WMS with 2f signals is employed to TDLAS[8–11] technique. There is now a general consensus that the first harmonic (1f) signal can be used to normalize the 2f signal to improve accuracy.[12,13] In these studies, the phase shift (PS) between the intensity and the wavelength modulation has been demodulated to optimize the 2f/1f fitting.[12] Although this method can reduce the detection error, it is intricate to demodulate the phase shift and use the simulated line shape to satisfy the best fitting.

In this paper, we derive the expressions of the 2f signal according to the absorption spectral and lock-in theories. By analyzing the expression of 2f signal with a different way of Fourier expansion (by putting the PS to the wavelength modulation and separating it from wavelength modulation frequency without as a whole in the process of Fourier expansion), we will research the influence factors of a 2f signal. In particular, the influences of PS (varies from 0.5π to π) and pressure are analyzed and simulated. The scope of this research lies in ambient pressure, temperature suppression, and phase shift effects elimination. Therefore, we have utilized a self-calibration WMS measurement method based on TDLAS with an advanced gas flow cell and a reference cell to detect the gas concentration. The selected 2f signal pairs of measured and reference WMS-2f spectra are used for 2f peak calibration, combining the advantage of concentration least-squares algorithm optimization, leading to high accuracy and linearity concentration detection. In addition, the transition of C_2H_2 at 1530.36 nm is selected based on the Pacific Northwest National Laboratory (PNNL) spectra database and spectral data from experiment. The numerical results calculated by new method are compared with conventional results (extract concentration from 2f signal peak without reference 2f signal calibration). The accuracy and linearity, precision and stability, detection limit and sensitivity are evaluated to verify the performance of the self-calibration system for simultaneous measurements of C_2H_2.

2. Measurement principles

2.1. Theoretical principles

Once the monochromatic radiation of the light source overlaps with a rotation transition of a gas species, absorption will occur, resulting in the attenuation of light intensity. The

*Project supported by the National Natural Science Foundation of China (Grant Nos. 61172047, 61502538, and 61501525).

†Corresponding author. E-mail: xuxuemei999@126.com

© 2016 Chinese Physical Society and IOP Publishing Ltd

transmitted intensity $I_t(v)$ at simultaneous time t associated with a rotation transition in a gas cell is given by the Beer–Lambert law, when the absorbance is lower than 5%,[13]

$$I_t(v) = I_0(v)\exp(-\alpha(v)PCL), \tag{1}$$

where $I_0(v)$ is the incident laser intensity at the laser center frequency v (cm^{-1}), P (atm) is the total measurement gas pressure, C is the mole fraction of the absorbing gases, L (cm) is the absorption path length, $\alpha(v)$ is the absorption coefficient which is related to line-strength $S(T)(\mathrm{cm}^{-2}\cdot\mathrm{atm}^{-1})$ and line-shape $g(v)$ (cm). Therefore, the Beer–Lambert law can be written as

$$I_t(v) = I_0(v)\exp(-S(T)PCLg(v)), \tag{2}$$

where $\alpha(v)$ has been replaced by $S(T)g(v)$. In the case of low-concentration detection, $S(T)PCLg(v) \ll 1$, equation (2) can be expanded by a first-order Taylor series, as follows:

$$\begin{aligned} I_t(v) &\approx I_0(v)(1 - S(T)PCLg(v)) \\ &= I_0(v)(1 - \varepsilon Cg(v)), \end{aligned} \tag{3}$$

where $\varepsilon = S(T)PL$. For a gas absorption line under regular pressure and temperature, the Lorentz line-shape function is adopted as[14]

$$g(v) = \frac{1}{\pi}\frac{\Delta v}{(v - v_0)^2 + \Delta v^2}, \tag{4}$$

where v_0 and Δv are the center wavelength and the half width at half-maximum (HWHM) of specific absorption line, respectively.

Compared with direct absorption measurements, WMS can improve the SNR and is less influenced by non-absorption transmission losses. In this paper, a saw tooth wave signal as well as a sine wave signal is injected into the distributed feedback laser (DFB) to tune the output wavelength. Getting the instantaneous center wavelength and laser intensity as follows:[10]

$$v = v_1 + a\cos(\omega t + \psi), \tag{5}$$

$$I_0 = I(v_1)[1 + i_0\cos(\omega t)], \tag{6}$$

where v_1 and $I(v_1)$ are the center wavelength and laser intensity of the passed light beam without modulation, respectively, a is the modulation depth, i_0 is the amplitude of linear laser intensity modulation, and ψ is the PS. Thus, equation (3) can be rewritten as

$$\begin{aligned} I_t &= I_0(1 + i_0\cos(\omega t + \psi_1))[1 - \varepsilon Cg(v_1 + a\cos(\omega t + \psi))] \\ &= I_0(1 + i_0\cos(\omega t + \psi_1)) \\ &\quad \times \left[1 - \varepsilon C\left(H_0 + \sum_{n=1}^{\infty} H_{\mathrm{na}}\cos(n\omega t) + H_{\mathrm{nb}}\sin(n\omega t)\right)\right], \end{aligned} \tag{7}$$

where $g(v_1 + a\cos(\omega t + \psi))$ has been expanded in Fourier series.[15] Here, we do not treat $(\omega t + \psi)$ as a whole during the Fourier expansion, as in previous Fourier analysis, so $\cos(\omega t + \psi)$ is not an even function of time t, and there will be two kinds of Fourier coefficients H_{na} and H_{nb}. However, it is less complicated when extracting the 2f components in Section 2.2, without decomposing $\cos(n(\omega t + \psi))$ parts. Fourier coefficients of H_0, H_{na}, and H_{nb} are given by

$$H_0 = \frac{1}{2\pi}\int_{-\pi}^{\pi}\frac{1}{\pi}\frac{\Delta v}{[v_1 + a\cos(\omega t + \psi) - v_0]^2 + \Delta v^2}t\mathrm{d}\omega, \tag{8}$$

$$\begin{aligned} H_{\mathrm{na}} &= \frac{1}{\pi}\int_{-\pi}^{\pi}\frac{1}{\pi}\frac{\Delta v}{[v_1 + a\cos(\omega t + \psi) - v_0]^2 + \Delta v^2} \\ &\quad \times \cos(n\omega t)t\mathrm{d}\omega, \end{aligned} \tag{9}$$

$$\begin{aligned} H_{\mathrm{nb}} &= \frac{1}{\pi}\int_{-\pi}^{\pi}\frac{1}{\pi}\frac{\Delta v}{[v_1 + a\cos(\omega t + \psi) - v_0]^2 + \Delta v^2} \\ &\quad \times \sin(n\omega t)t\mathrm{d}\omega. \end{aligned} \tag{10}$$

According to the statement of basic measurement principles, various influence factors of 2f signals including the pressure and PS ψ are investigated. This will be followed by descriptions of Simulink results and detailed presentations of how the 2f signals are affected.

2.2. Influence factors of 2f signals

Wavelength-scanned and wavelength-modulation spectroscopy with 2f signal detection is used to determine the absorption magnitude and gas concentration in actual measurements. To find out the influence factors of 2f signals' peaks, the expressions of the 2f signals are further derived by Eq. (7). Therefore, assuming that the expression of the second components of the transmitted intensity I_t can be written as

$$I_{2\omega} = F_{21}\cos(2\omega t) + F_{22}\sin(2\omega t), \tag{11}$$

where F_{21} and F_{22} are given by

$$\begin{aligned} F_{21} &= -\varepsilon CI_0\left[H_{2\mathrm{a}} + \frac{i_0}{2}(H_{1\mathrm{a}} + H_{3\mathrm{a}})\right], \\ F_{22} &= -\varepsilon CI_0\left[H_{2\mathrm{b}} + \frac{i_0}{2}(H_{1\mathrm{b}} + H_{3\mathrm{b}})\right]. \end{aligned} \tag{12}$$

A lock-in amplifier (LIA) is used to shift the 2f signal components from 2f frequency to zero frequency, by multiplying the transmitted laser intensities I_t by $\cos(2\omega t)$ for the $X_{2\mathrm{f}}$ component and $\sin(2\omega t)$ for the $Y_{2\mathrm{f}}$ component. A numerical low-pass filter with a bandwidth less than f/2 is then used to extract these components. As a result, the alternating current (AC) signals are removed and the direct current (DC) signals are remained as follows:

$$\begin{cases} X_{2\mathrm{f}} = GRF_{21}, \\ Y_{2\mathrm{f}} = GRF_{22}, \end{cases} \tag{13}$$

where G is the electro–optical gain of the measurement system and R is the amplification factor of the reference signals.

According to Ref. [13], we know that the values of odd harmonics at the line center are always approximately zero and the values of even harmonics are always maxima. Considering that the influences of PS ψ to odd harmonics are extremely small, we regard that $H_{1a} = H_{1b} = H_{3a} = H_{3b} \approx 0$. Therefore, the X_{2f} and Y_{2f} components can be simplified as follows:

$$\begin{cases} X_{2f} = -GRI_0\varepsilon CH_{2a}, \\ Y_{2f} = -GRI_0\varepsilon CH_{2b}. \end{cases} \tag{14}$$

The absolute peak S_{2f} of the 2f signal is then given as

$$S_{2f} = \sqrt{X_{2f}^2 + Y_{2f}^2} = GRI_0\varepsilon C\sqrt{H_{2a}^2 + H_{2b}^2}. \tag{15}$$

Obviously, the absolute peak S_{2f} is determined by the ambient pressure, temperature, laser intensity, H_{2a} and H_{2b}. As noted, H_{2a} and H_{2b} are much dependent on the PS between the intensity and the wavelength modulation. The PS ψ is determined by contributions from two effects, namely: slow thermal mechanisms and fast carrier injection effects.[16] (I) The thermal effect (the expansion of the optical path length in the DFB laser grating period) produces an increase in the wavelength with the current. At high modulation frequency, thermal delay causes that the wavelength modulation progressively lags the intensity modulation. (II) Carrier injection, through plasma and band filling effects, decreases the wavelength as the current increases. The wavelength modulation from this effect is π out of phase from intensity modulation. As illustrated in Fig. 1, the PS ψ can be any value from 0.5π to π. This will make great changes to the values of H_{2a} and H_{2b}, resulting in the fluctuation of S_{2f}.

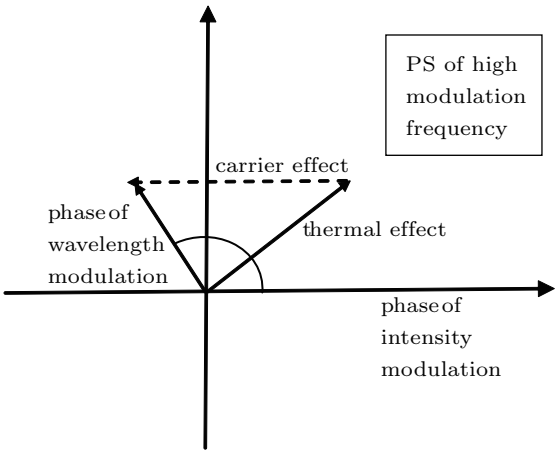


Fig. 1. Illustration of PS in a DFB laser diode for high modulation frequency.

Beyond that, the line-width of DFB laser also contributes a lot to the 2f signal peak. The peak expressions of 2f signal derived above have assumed that the line-width is zero, which cannot describe how DFB laser line-width affects the 2f signal peak. Here, we assume that the DFB line-width is v,[17] and then the output intensity of line-center v_0 is

$$I_0(v_0) = \int_{v_0 - v/2}^{v_0 + v/2} I(v)\,\mathrm{d}v. \tag{16}$$

In this way, the adjusted $S_{2f}(v_0)$ can be expressed as

$$S_{2f}(v_0) = GR\varepsilon C\int_{v_0 - v/2}^{v_0 + v/2} I(v)\sqrt{H_{2a}^2 + H_{2b}^2}\,\mathrm{d}v. \tag{17}$$

Here, more than one wavelength is involved in the absorption of the intensity when the line-width v exists. However, the absorption coefficients of the wavelengths on both sides of the line-center are smaller than $\alpha(v_0)$. Besides, when the line-center of the wavelength is farther away, the absorption coefficient is smaller. Accordingly, this causes the $\sqrt{H_{2a}^2 + H_{2b}^2}$ of the wavelengths on both sides of the line-center to be smaller. Therefore, for the same intensity of $I_0(v_0)$, the peak of 2f signal increases as the line-width decreases. As a result, the measurement results are more accurate with a narrower DFB laser line-width. Practically, the DFB line-width utilized here is approximately 2 MHz (1.56×10^{-5} nm), which means that we can treat it as a monochromatic light with zero line-width.

Moreover, temperature variation only affects the line-strength $S(T)$, and line-strength has a negative linear correlation relationship with temperature. According to this negative linear correlation relationship and Eq. (15), the 2f signal peak also has a negative linear correlation relationship with temperature, which agrees very well with the conclusion in Ref. [18]. Hence, the issue of the effect of temperature on the measurement results is not involved in this paper.

To verify the correctness of the proposed idea, a platform based on Matlab Simulink is established and the effectiveness of pressure and phase shift to peaks of 2f signals is analyzed. Here, the parameters of simulation conditions are similar to the parameters of the practical measurements. The gas temperature and absorption path length are 296 K and 40 cm, respectively. Meanwhile, the gas pressure varies from 0.8 atm to 1.2 atm,[19] and the PS ψ varies from 0.5π to π. The simulation results are shown in Figs. 2 and 3.

The 2f signals under different pressures (assuming the PS $\psi = 0$, $T = 296$ K) are shown in Fig. 2(a) and 2f signals under different PSs (assuming the pressure $P = 1.0$ atm, $T = 296$ K) are shown in Fig. 2(b). The absolute peaks of 2f signals are shown in Fig. 3 to make the diagram more intuitive, where peaks vary with pressure and PS ψ. The simulation results indicate that the peaks of 2f signals decrease with the increase of pressure. In contrast, the peaks may be unpredictable and uncertain because the PS ψ might be any value from 0.5π to π and light intensity fluctuates during the measurement. In consideration of this, self-calibration WMS with reference 2f signal calibration is applied to TDLAS to improve the detection accuracy in the next section.

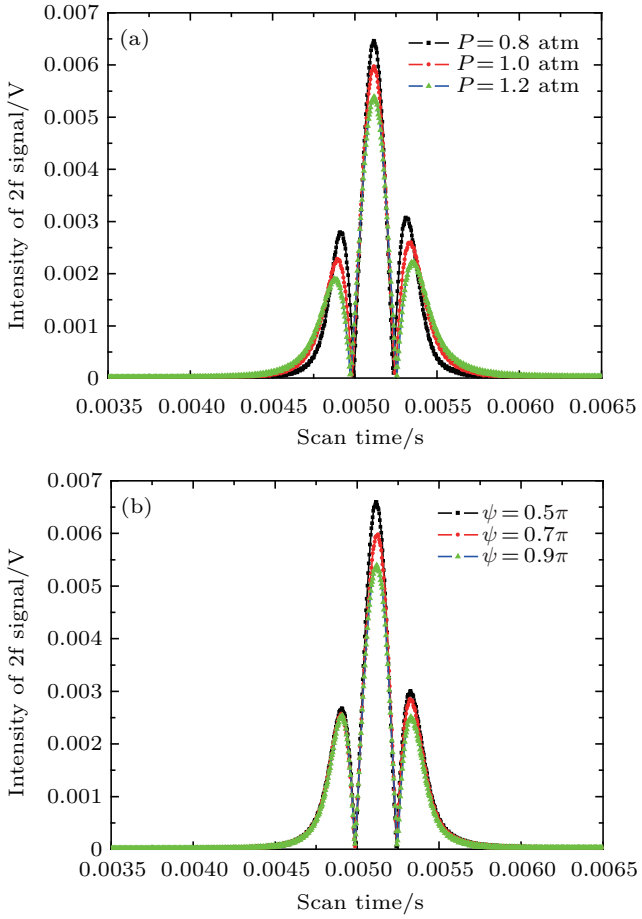


Fig. 2. (color online) The 2f signals under different pressures (assuming $\psi = 0$, $T = 296$ K) (a) and under different phase shifts (assuming $p = 1.0$ atm, $T = 296$ K) (b).

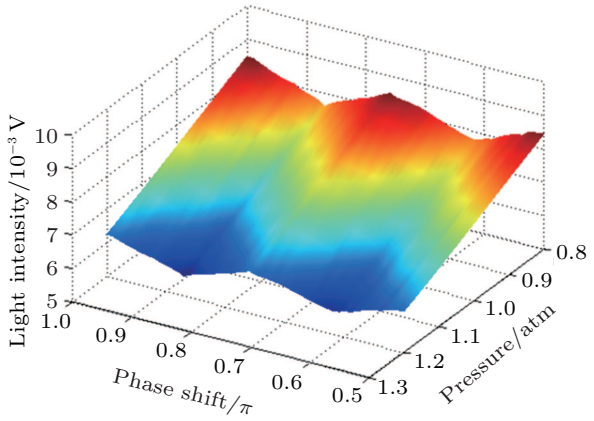


Fig. 3. (color online) Peaks of 2f signals under different pressures and phase shifts.

3. Scheme of the self-calibration WMS system

A self-calibration WMS experimental system is developed based on TDLAS, as shown in Fig. 4. For trace measurement, a DFB diode laser with an emission wavelength from 1529 nm to 1531 nm (customized by SCTG Company) and a diode-laser controller (SDDT-T-x-MA) is used as a light source. It is difficult to keep the optical wavelength of the DFB at line center because of the fluctuation of outside temperature and the slight drift of the oscillation current. The wavelength-sweep technique and WMS are employed to detect the absorption line with a low-frequency scanning signal and high-frequency sinusoidal modulation signal, respectively, as the laser drive current. Furthermore, a 1-in-2 (50:50) coupler is applied to divide the transmission light from the DFB into two equal parts. One passes through the measurement gas cell (fiber-coupled flow-cell) which contains gases needed to be measured, and the signal beam irradiated onto an InGaAs photo-detector 1 (PD1). The other one passes through the reference gas cell (C_2H_2 standard pressure cell), which contains the same kind of gases with known concentration, and the signal beam is irradiated onto an InGaAs photo-detector 2 (PD2). The outputs of PD1 and PD2 are connected to the LIA as inputs. With the help of the reference signal of sinusoidal wave at 50 kHz, the LIA demodulates the input signals into 2f signals. Finally, the 2f signals are captured by a PC for data processing.

A self-calibration scheme is introduced into the gas concentration experimental with a reference gas cell. The reference gas cell and the measurement gas cell share the same kind gas but with different concentrations. They are placed under the same ambient temperature and pressure. Referring to Eq. (15), we known that

$$S_{2f,test} \propto I_{0,test} P_{test} C_{test} L_{test} S(T_{test}) \left(\sqrt{H_{2a}^2 + H_{2b}^2}\right)_{test}, \quad (18)$$

$$S_{2f,ref} \propto I_{0,ref} P_{ref} C_{ref} L_{ref} S(T_{ref}) \left(\sqrt{H_{2a}^2 + H_{2b}^2}\right)_{ref}, \quad (19)$$

where $S_{2f,test}$ and $I_{0,test}$ are the 2f signal and input intensity of measurement gas cell, P_{test}, C_{test}, and L_{test} are the pressure, gas concentration, and absorption path length of measurement gas cell respectively, $S(T_{test})$ is the line-strength at the temperature of T_{test}, and $\left(\sqrt{H_{2a}^2 + H_{2b}^2}\right)_{test}$ is related to the PS ψ of measurement gas cell. Similarly, the parameters of reference gas cell in Eq. (19) are consistent with the parameters of measurement gas cell in Eq. (18).

For an exact optical fiber gas concentration detection system, the absorption path length is known. The light beams in the two paths separated by the coupler are of the same intensity and PS ψ between the wavelength modulation and intensity modulation. Such an operation devotes the proportion of $\left(\sqrt{H_{2a}^2 + H_{2b}^2}\right)_{test}$ and $\left(\sqrt{H_{2a}^2 + H_{2b}^2}\right)_{ref}$ is immune to fluctuation caused by PS ψ. In order to minimize the influence of temperature, the temperature of the measurement and reference cells are kept equal to room temperature during the experiment. For pressure, the difference pressures between measurement and reference gas cells will lead to different line-broadenings and line shapes. In terms of the Lorentz line-shape which is chosen for absorption principle analysis and Fourier expansion above, the pressure for the best line-shape fitting needs to be maintained between around 0.8 atm and 1.2 atm.[19] Simulations in Fig. 2(a) demonstrate that the 2f

signal peak decreases as the pressure increases. Here, an optimum pressure of 0.8 atm is selected for measurement and reference gas cells. Hence, the influence of temperature and pressure drift on the two light paths should be very similar. The difference between the two light paths approaches zero. Under these circumstances, the calculation method of gas concentration can be expressed as

$$C_{\text{test}} = \frac{S_{\text{2f,test}} C_{\text{ref}} L_{\text{ref}}}{S_{\text{2f.ref}} L_{\text{test}}}. \tag{20}$$

This is able to efficiently suppress the peak fluctuations of 2f signals induced by pressure, temperature, PS ψ, and light intensity.

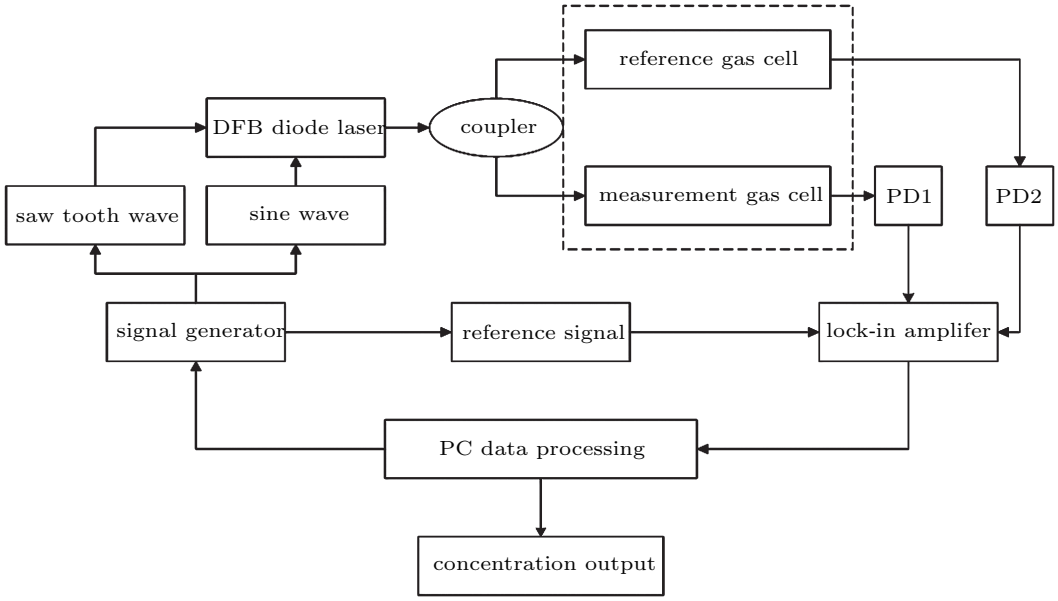


Fig. 4. Scheme illustration of the self-calibration experimental system.

4. Concentration measurement results and discussion

4.1. Measurement of PS ψ

The PS ψ has been measured to proof and express the correctness of the proposed theory in Section 2.2. A 0.016-cm^{-1} FSR etalon is utilized as the substitute of reference gas cell to record the relative wavelength variation accurately. The PS is extracted as shown in Fig. 5(a) from the measured modulation of wavelength and intensity. When the laser injection current is sinusoidal-modulated, the light intensity is nearly simultaneously modulated, but some delay is observed in wavelength response. As illustrated in Fig. 5(a), this PS between wavelength and intensity modulation is 0.65π at a modulation frequency of 25 kHz. More PSs that have been measured at different modulation frequencies are shown in Fig. 5(b). As the modulation frequency increases, the PS increases slowly, this coincides with our theoretical analysis. Fortunately, the PS influence can be eliminated by the self-calibration method described below.

4.2. Selection of C_2H_2 absorption line

The choice of C_2H_2 absorption line needs to fulfill the following requirements: (i) the absorption line is strong at the measurement temperature (near 300 K), providing good SNR

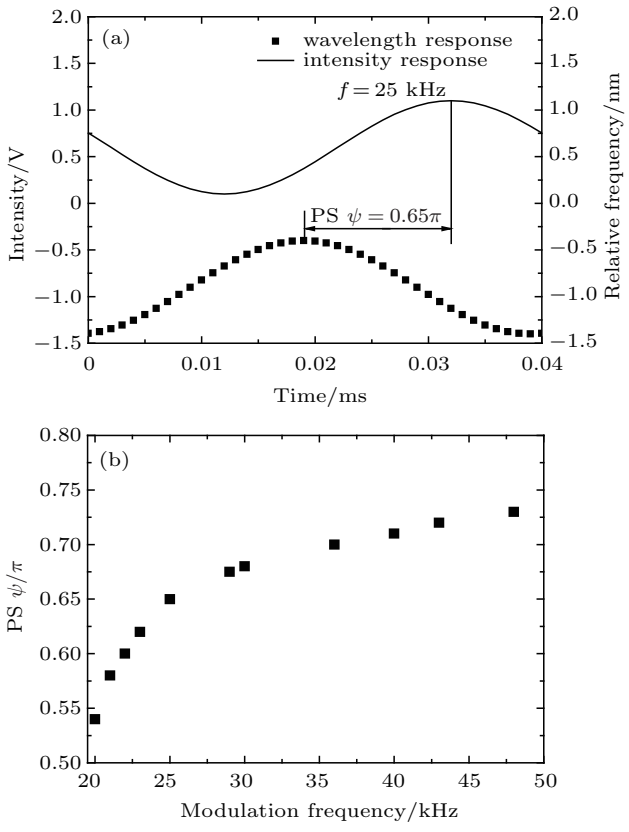


Fig. 5. Schematic for measuring wavelength and intensity modulation PS at 25 kHz (a) and different frequencies (b).

and measurement precision; (ii) the transition is well isolated from neighbors and other gases; and (iii) the collisional width is small, providing narrow line-shape to enhance WMS signals. The DFB diode laser applied here possesses an operating center wavelength near 1530 nm. It means that a C_2H_2 absorption line near 1530 nm needs to be chosen. Figure 6(a) presents the C_2H_2 absorption lines of PNNL database at 296 K near 1530 nm. The figure suggests that the absorption line in the red rectangular box with the maximum intensity should be chosen. Here, we set the linear sweep wavelength from 1530.0 nm to 1530.8 nm with a precision of 0.004 nm/mA to detect the absorption line in our experiment. Figure 6(b) shows that the absorption line detected from the experiment without wavelength modulation contains exactly one complete absorption line. Therefore, in our experiment, the absorption line center at 1530.36 nm of the highest absorption point within the spectral range of the DFB is chosen.

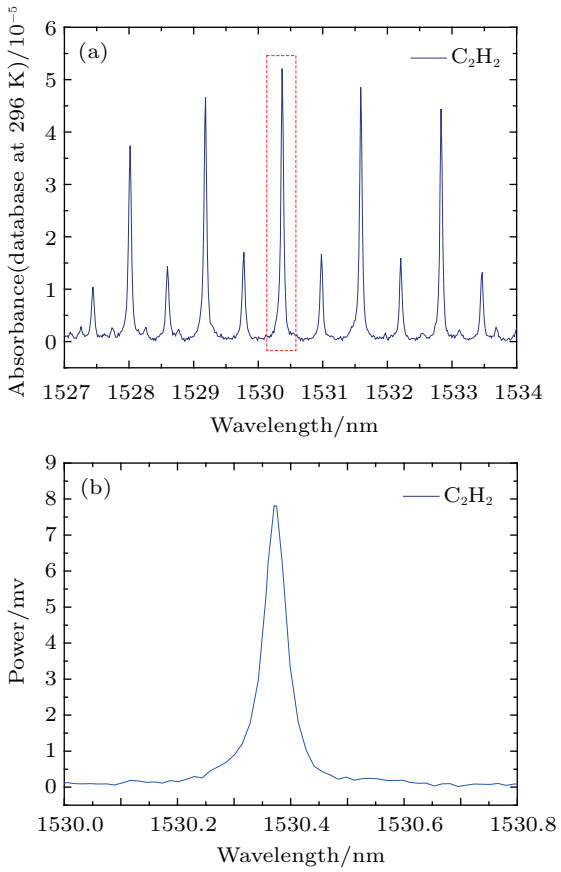


Fig. 6. (color online) C_2H_2 absorption lines of PNNL database at 296 K (a) and experiment (b).

4.3. Measurements of C_2H_2 concentration

In the experiment, the reference gas cell (40-cm long with a fixed pressure of 0.8 atm) is contained with standard C_2H_2 gas of 100-ppmv concentration. A fiber-coupled gas flow cell (FC-16 FCM, 40-cm long) is employed as the measurement gas cell. The measurement gas is C_2H_2 with a concentration range of 0 ppmv–400 ppmv. The total pressure in the gas flow cell is also kept at $\sim$ 0.8 atm to minimize the line shape discrepancies between the measurement and reference 2f signals. The gas pressure of the measurement gas cell is measured and controlled by vacuum pressure gauge (BST-111) with an accuracy uncertainty of 0.01%. The laser wavelength is driven by a 30-Hz saw tooth wave summed in an adder with a 25-kHz sine wave to provide the wavelength modulation. Before each measurement, the gas sample was allowed to stabilize thermally with enough time. In this way, the temperatures of the two gas cells can be kept at room temperature and the influence of temperature can be minimized.

Examples of experiment measured 2f signals of detecting the 50-ppmv and 100-ppmv C_2H_2 standard gases under the pressure of 0.8 atm are shown in Figs. 7(a) and 7(b). We choose the 100-ppmv C_2H_2 standard gas as the reference gas. Background measurements without C_2H_2 absorption caused by and directly proportional to the laser intensity and the electronic gain, are conducted to normalize and correct the 2f signals.

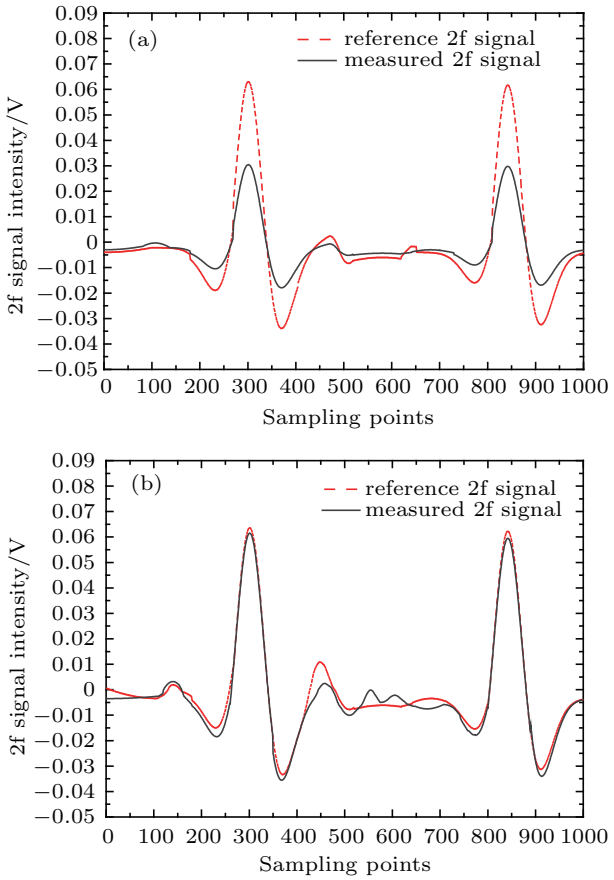


Fig. 7. (color online) Measured and reference 2f signals of 50-ppmv C_2H_2 gases (a) and 100-ppmv C_2H_2 gases (b).

To guarantee the extracted concentration accuracy of the measurements, only 2f signal pairs with highly consistent line shapes between measured and reference 2f signals are applied. The useful signal pairs are selected by comparing the HWHMs of measured and reference 2f absorbance spectra.

The convenient and reliable data processing method is based on peak-trough seeking algorithm, and then extracting the relative HWHMs through the difference sampling points between peak and trough of measured and reference 2f signals. The selected signal pairs can be used to derive the C_2H_2 concentrations in the measurement gas cell from the normalized measured and reference 2f signal intensities' peak heights according to Eq. (20). The measured concentrations are optimized by linear-fitting between the measured and reference signal pairs based on a least-squares algorithm. In Fig. 8, the slope of the fitting line represents the concentration ratio of the gases in the measurement and reference gas cells after normalizing their 2f signal intensities' peak heights. From the slope in Fig. 8, we can calculate the optimized C_2H_2 concentration in the measurement gas cell is 50.36 ppmv. The high value of correlation coefficient (R^2) confirms the feasibility of the data processing method.

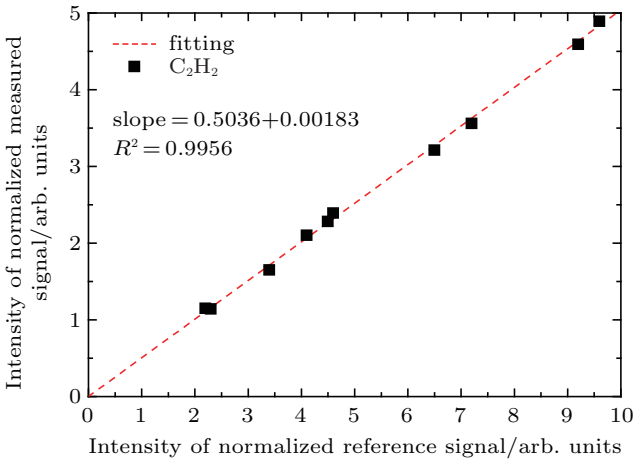


Fig. 8. (color online) Selected data points (normalized intensities) of measured and reference signal pairs and linear fitting for C_2H_2 concentration optimization.

Besides, 100-ppmv, 200-ppmv, and 400-ppmv C_2H_2 standard gases are detected to verify the accuracy and linearity of the self-calibration method. Figure 9 shows the scatter plot and linear fitting of measured concentration of C_2H_2 versus the known concentration values in the range of 0–400 ppmv. The figures demonstrate that the measured C_2H_2 concentrations from the self-calibration method are in good agreement with the known concentrations over the entire concentration range. The correlation coefficient ($R^2 = 0.9983$) of those measured concentration points indicates the good linearity of this self-calibration method. Table 1 shows the comparison of measurement results obtained using self-calibration method and conventional method. Table 1 reveals that the self-calibration method has a lower error rate than the conventional method, especially at low C_2H_2 concentration conditions. For instance, when measuring the 50-ppmv standard gases, the error rate without reference gas cell is 7.36% but the self-calibration method is only 0.72%, and then leads to a high measurement accuracy with the advantages of ambient pressure, temperature suppression, and phase shift influences elimination. The overall comparison demonstrates the feasibility of using the reference 2f signal-calibration method for determination of C_2H_2 concentration, which owns good accuracy and linearity without the necessity of demodulating the PS ψ to improve the detection precision.

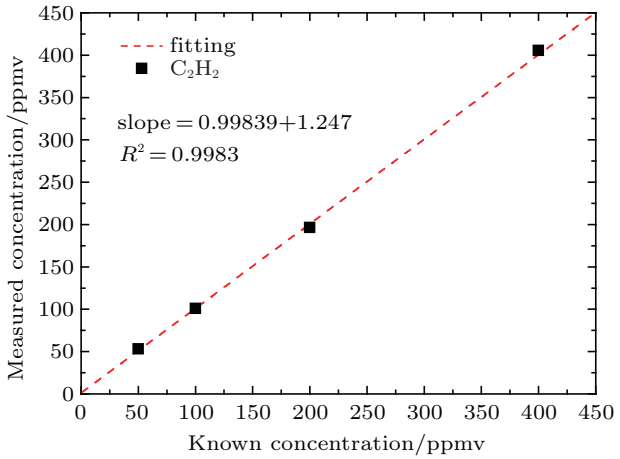


Fig. 9. (color online) Comparisons of the measured concentrations of C_2H_2 versus the known values in the range of 0–400 ppmv.

Table 1. Comparison of measurement results of self-calibration method and conventional method.

Known concentrations of C_2H_2/ppmv	Measurement results of self-calibration method		Measurement results without reference gas cell	
	Concentration/ppmv	Error/%	Concentration/ppmv	Error/%
400.00	401.13	0.283	405.31	1.327
200.00	198.94	0.53	194.87	2.565
100.00	100.65	0.65	104.14	4.14
50.00	50.36	0.72	53.68	7.36

4.4. System stability analysis

The stability of the instrument performance is analyzed based on the standard deviation. When the standard deviation is lower, instrument performance will be better. After over 3 h, 50-ppmv C_2H_2 standard gas is measured to evaluate the stability, as shown in Fig. 10. The standard deviation of 50-ppmv C_2H_2 standard gas measured by self-calibration method is 0.431 ppmv, which is smaller than the conventional method of 1.415 ppmv. This suggests that the new self-calibration method with reference 2f signal calibration owns a quite better stability. The range of the results is 1.632–10.325 ppmv, which predicates that the precision of self-calibration method

is improved from around 10 ppmv to 1.6 ppmv. Obviously, the 1.6-ppmv precision is more accommodating for practical applications and the facility is equipped with an accurate C_2H_2 measurement for self-calibration.

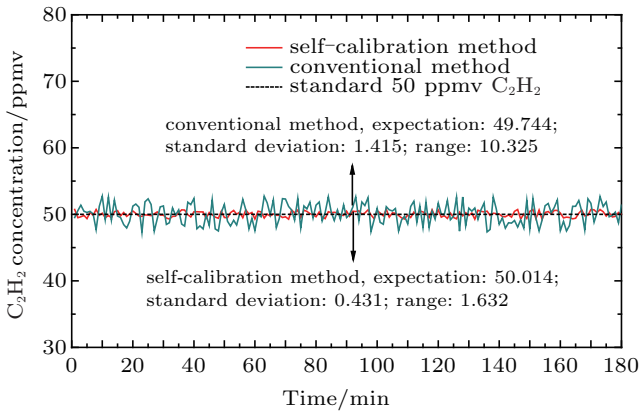


Fig. 10. (color online) Measurement results of 50-ppmv C_2H_2 standard gas for 3 h using self-calibration method and conventional method.

4.5. System detection limit and sensitivity

The detection limit of self-calibration detection system based on reference 2f signal calibration method is determined by Allan analysis.[20] Here, C_2H_2measurements with 5-ppmv standard gas are performed during an estimated 1-h experiment. An Allan variance is utilized to analyze the stability and detection limit of the system. Figure 11(a) exhibits the Allan variance as a function of the integration time t from the measurement concentrations. The Allan variance shows that a minimum detection limit of 122 ppbv can be achieved using an optimum integration time of 296 s. Hence, the high detection limit illustrates the high stability and performance of the developed self-calibration method. Moreover, the measured 2f signal in the measurement gas cell filled with 5-ppmv C_2H_2 is shown in Fig. 11(b). With the noise level of 0.193 mV in the base line and the peak heights of 6.3 mV of the measured 2f signal from the measurement gas cell, the SNR of approximately 32.6 is obtained.

Here, the sensitivity of self-calibration detection system is determined by the ratio of variation in output light intensity and variation in C_2H_2 concentration. It can be described as

$$k = \frac{\Delta I}{\Delta C}, \tag{21}$$

where k is the system sensitivity, ΔI is the variation in output light intensity, and ΔC is the variation in C_2H_2 concentration. According to Beer–Lambert law in Eq. (1),

$$\begin{aligned} I - \Delta I &= I_0[1 - \alpha(C + \Delta C)L] \\ &= I - I_0 \alpha \Delta C L, \end{aligned} \tag{22}$$

and then the sensitivity can be written as

$$k = \frac{\Delta I}{\Delta C} = I_0 \alpha L. \tag{23}$$

The light intensity of the DFB laser at 1530.36 nm without gas absorption is 4.316 mW. Under the pressure of 0.8 atm, the absorption coefficient of C_2H_2 gas molecule at the wavelength of 1530.36 nm is 0.628 cm^{-1} and the absorption path length is 40 cm. Consequently, the system sensitivity of 0.11 μW/ppmv is obtained from Eq. (23).

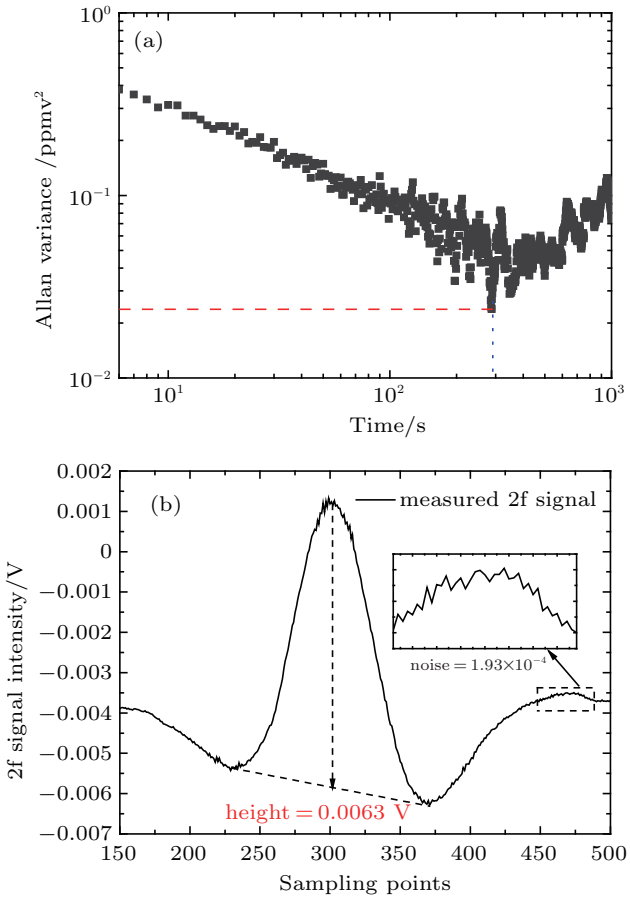


Fig. 11. (color online) Allan variance from time series measurements for 5-ppmv C_2H_2 (a) and measured 2f signal in the measurement gas cell (b).

5. Conclusion

In this paper, self-calibration wavelength modulation spectroscopy for acetylene detection based on TDLAS has been presented. The expressions of 2f signal are derived according to the absorption spectral and lock-in theories, where the 2f signal peak can be recurrently influenced by phase shift between the wavelength modulation and intensity modulation. Moreover, a self-calibration experimental system with reference 2f signal calibration method is designed. In our experiment, the influences of pressure, temperature, and phase shift on the measurement concentrations are suppressed markedly. The numerical results indicate that the self-calibration system performs better accuracy and stability than the conventional one. The precision of the system can reach 1.6 ppmv through standard deviation analysis. Furthermore, by conducting Allan variance analysis and absorption principle discussion, the detection limit and sensitivity of 122 ppbv and 0.11 μW/ppmv

have been achieved, respectively. This is significant for practical applications in many other gases.

References

[1] Duval M 1989 *IEEE Electr. Insul. Mag.* **5** 22
[2] Chen W, Zhou Q, Su X, Xu L and Peng S 2013 *Sensors Transducers* **154** 195
[3] Gondal M A, Dastageer A and Shwehdi M H 2004 *Talanta* **62** 131
[4] Liu K, Guo X Y, Yi H M, Chen W D, Zhang W J and Gao X M 2009 *Opt. Lett.* **34** 1594
[5] Liu A, Jones R, Liao L, Samara-Rubin D, Cohen O and Paniccia M 2004 *Nature* **427** 615
[6] Reid J and Labrie D 1981 *Appl. Phys. B* **26** 203
[7] Xia H, Dong F Z, Wu B, Zhang Z R, Pang T, Sun P S, Cui X J, Han L and Wang Y 2015 *Chin. Phys. B* **24** 034204
[8] Qu Z, Ghorbani R, Valiev D and Schmidt F M 2015 *Opt. Express* **23** 16492
[9] Bjorklund G C 1980 *Opt. Lett.* **5** 15
[10] Liu J T C, Jeffries J B and Hanson R K 2004 *Appl. Phys. B* **78** 503
[11] Iwamitsu K, Aihara S, Shimamoto T, Fujii A and Akai I 2012 *Rev. Sci. Instrum.* **83** 073101
[12] Salati S H and Alireza K 2014 *Appl. Phys. B* **116** 521
[13] Che L, Ding Y J, Peng Z M and Li X H 2012 *Chin. Phys. B* **21** 127803
[14] Wei W, Chang J, Huang Q, Zhu C, Wang Q, Wang Z and Lu G 2015 *Appl. Phys. B* **118** 75
[15] Cai W W and Kaminski C F 2014 *Appl. Phys. Lett.* **104** 154106
[16] Jacobsen G, Olesen H, Birkedahl F and Tromborg B 1982 *Electron. Lett.* **18** 874
[17] Chawki M J, Auffret R, Coquil E L, Pottier P, Berthou L, Paciullo H and Bihan J L 1992 *J. Lightwave. Technol.* **10** 1388
[18] Hu C, Chen X and Li Z 2015 *3rd International Conference on Material, Mechanical and Manufacturing Engineering (IC3ME* 2015), in *Advances in Engineering Research*, p. 1082
[19] Chen Z, Tao S H, Du X J and Hou X J 2013 *Spectrosc. Spect. Anal.* **33** 312 (in Chinese)
[20] Lewicki R, Doty J H, Curl R F, Tittel F K and Wysocki G 2009 *P. Natl. Acad. Sci.* **106** 12587